Carbohydrate Polymers 82 (2010) 989–996

Contents lists available at ScienceDirect

Carbohydrate Polymers

journal homepage: www.elsevier.com/locate/carbpol

# Biohybrid barrier films from fluidized pectin and nanoclay

Jari Vartiainen*, Tekla Tammelin, Jaakko Pere, Unto Tapper, Ali Harlin

*VTT Technical Research Centre of Finland, P.O. Box 1000, FI-02044 VTT, Finland*

ARTICLE INFO

*Article history:*
Received 1 February 2010
Received in revised form 14 June 2010
Accepted 18 June 2010
Available online 1 July 2010

*Keywords:*
Pectin
Nanoclay
Film
Barrier
Biopolymer

ABSTRACT

The work was aimed at studying the effects of nanosized montmorillonite on the barrier properties of the unmodified sugar beet pectin films as a function of relative humidity. 0.5, 1 or 2 wt% nanoclay was dispersed in an aqueous 5 wt% pectin solution using high pressure fluidizer. Nanoclay-pectin hybrid film formation and high shear induced orientation of nanoclay platelets were investigated by means of model surfaces which were prepared using high shear spincoating. After fluidization, the nanoclay formed uniform and laterally oriented stacks consisting of approximately 15 individual nanoclay layers. Pectin films with the final nanoclay concentrations of 0, 10, 20 and 30 wt% were prepared by casting. Nanocomposite films made of pectin and montmorillonite showed improved barrier properties against oxygen, and water vapour. Films were also totally impermeable to grease. The developed biohybrid material can be potentially exploited as a safe and environmentally sound alternative for synthetic barrier packaging materials.



## 1. Introduction

There is a growing interest in utilization of by-products of agriculture and food industry in order to develop biodegradable materials to replace petroleum based polymers in packaging applications. In addition, nanotechnology in food packaging is expected to grow strongly over the next five years as the increased globalization sets demands for shelf life enhancing packaging. Applications of nanotechnology include improved barrier, mechanical and antimicrobial properties, as well as the incorporation of nanosensors for traceability and the monitoring the condition of foodstuffs during transport and storage (Harrington, 2009). In recent years a lot of effort has been aimed at developing new biobased polymer containing films and nanocomposites which can act as barrier materials in packaging applications (Arora & Padua, 2010; Bae, Park, Darby, Kimmel, & Whiteside, 2009; Lagarón & Fendler, 2009; Maksimov, Lagzdins, Lilichenko, & Plume, 2009; Mangiacapra, Gorrasi, Sorrentino, & Vittoria, 2006; Napierała & Nowotarska, 2006; Plackett et al., 2006; Vartiainen et al., 2010).

Unlike synthetic plastics, in dry conditions the films of natural polymers exhibit good barrier properties against oxygen and grease due to the high amount of hydrogen bonds in their structure. However, natural polymers are hydrophilic in nature and films produced from these materials are often hygroscopic, resulting in partial loss of their barrier properties at high humidity. The gas permeability of polysaccharide materials may increase manifold when humidity increases (Hansen & Plackett, 2008). Since most of the food applications demand materials that are resistant to moisture as well, the major challenge is to overcome the inherent hydrophilic behaviour of these biomaterials (Bae et al., 2009).

Pectin is a structural heteropolysaccharide found in the primary cell walls of terrestrial plants and it has a complex structure. Pectin, when extracted from higher plants, contains smooth (linear) regions and hairy, branched regions. The linear, smooth regions are made up of α-(1-4)-linked D-galacturonic acid residues, some of which are methylesterified. The hairy region contains a backbone of the repeating disaccharide (→4)-α-D-GalpA-(→2)-α-L-Rhap-(→). The Rhap residues are substituted at C-4 with neutral oligosaccharide side chains composed mainly of arabinose and galactose residues. In sugar beet pectin these arabinose and galactose residues in the neutral sugar side chains are substituted by ferulic acid residues linked at C-2 (arabinose) or C-6 (galactose) positions (Siew & Williams, 2008). The degree of esterification, describing the percentage of acid group present in the ester form, determines the solubility of pectin and it's gelling and film forming properties and hence it's industrial applicability to a large extent. The degree of methylesterification varies with the origin of the plant source and the processing conditions e.g. storage, extraction, isolation and purification (Kirby, MacDougall, & Morris, 2008; Vincken et al., 2003; Zsivánovits, Marudova, & Ring, 2005). From a physico-chemical point of view pectin is an anionic polyelectrolyte, thus ionic interactions have a big impact on its behaviour in dispersions with nanoclays.

Frequently applied method to improve the strength and water resistance as well as barrier properties of the natural polymers is to blend them with inorganic fillers. These hybrid organic–inorganic

* Corresponding author. Tel.: +358 0 20 722 6188.
*E-mail address:* jari.vartiainen@vtt.fi (J. Vartiainen).

0144-8617/$ – see front matter © 2010 Elsevier Ltd. All rights reserved.
doi:10.1016/j.carbpol.2010.06.031

systems, especially those in which the inorganic material is dispersed in a polymeric matrix at a nanometric level have reported to possess enhanced strength, stability and barrier characteristics (Pavlidou & Papaspyrides, 2008). Nanolayered silicates such as hectorite, saponite and montmorillonite have attracted a particular interest due to their high performance at low filler loadings, rich intercalation chemistry, high surface area, high strength and stiffness, high aspect ratio of individual platelets, abundance in nature, and low cost (Blumstein, 1965; Lan, Kaviratna, & Pinnavaia, 1994; Messersmith & Giannelis, 1995; Yano, Usuki, & Okada, 1997). Due to their unique plate-like structure and high aspect ratio, nanoclays can effectively increase the tortuosity of the diffusion path of the diffusing molecules. Thus significant improvement in barrier properties can be achieved with the addition of relatively small amounts of clays (Pavlidou & Papaspyrides, 2008).

The nanoclay, montmorillonite, used in this work belongs to the group of dioctahedral smectites (2:1 phyllosilicates) and it has the following general composition: $(M^{+}_{y}{\cdot}nH_2O)((Al^{3+}{}_{2-y}Mg^{2+}{}_{y})Si_4{}^{4+}O_{10}(OH)_2)$ where $M^{+}$ refers to a generic monovalent interlayer cation. Layer thickness of the smectites is approximately 1 nm whereas the lateral dimensions of the platelets may vary within 0.1–1.0 μm. Therefore the aspect ratio (ratio of the particle width to its height) of the platelets can vary within 100–1000. Smectites carry a total negative layer charge of 0.2–0.6 equiv./formula unit $(Si,Al)_4O_{10}$. For montmorillonites the layer charge is typically around 0.3 equiv./formula unit corresponding to a 0.10 $Cm^{-2}$. The overall negative charge is balanced by sodium and calcium ions (exchangeable cations) which exist hydrated in the interlayer. The layers are held together by relatively weak electrostatic forces between layers and interlayer cations and thus, water and other polar molecules can enter between the unit layers leading to expansion of the lattice structure. The strength of the attraction is dependent on the charge density of the layers.

The surface charge on the faces of the clay particles is permanently negative whereas the sign and charge density at the edges depend on the pH of the dispersion. The charging arises from adsorption or dissociation of protons in the case of oxides. In an acidic medium an excess of protons creates positive edge charges which density decreases with increasing pH. Negative charge is produced by the dissociation of silanol and aluminol groups (Tournassat, Ferrage, Poinsignon, & Charlet, 2003; Tournassat, Greneche, Tisserant, & Charlet, 2003). Due to the different types of the charges present on the nanoclay particle surfaces the coagulation of the particles is strongly dependent on pH and ionic strength of the dispersion as well as on charge density of nanoclay particles. Aqueous dispersions of nanoclays spontaneously coagulates at pH < 4 due to the electrostatic attraction of the oppositely charged surfaces. At pH < 6 coagulation occurs at small salt concentrations especially when the surface charge density is low.

Hydrophilic nanoclay particles can be dispersed relatively easily into the hydrophilic natural polymer matrix, especially when the sufficient amount of mixing energy is used. When the clay layers are completely and uniformly dispersed in a continuous polymer matrix, exfoliated or delaminated structures are obtained. Intercalated structures are formed when extended polymer chains are intercalated between the silicate layers resulting in a well ordered multilayer structure of alternating polymeric and inorganic layers, with a repeat distance between them (Pavlidou & Papaspyrides, 2008).

The main goal of this work was to see the improved effect of nanosized montmorillonite on the barrier properties of the unmodified sugar beet pectin films as a function of relative humidity. Although similar kinds of hybrid films with natural polymers and nanoclay and their barrier properties have been extensively reported (Pavlidou & Papaspyrides, 2008), to our knowledge, this is the first time when the dispersing of the natural polymer-nanoclay fluids has been conducted using the high pressure fluidizer. Deeper structural and morphological understanding of the nanoclay-pectin film formation and nanoclay orientation on the solid surfaces were investigated via model surfaces prepared by high shear spin coating method. The model film structures were investigated by means of atomic force microscopy (AFM) and scanning electron microscopy (SEM). In addition, structure and morphology of the solvent cast films were investigated by SEM, X-ray diffraction (XRD) measurements and profilometric studies. Finally, the oxygen, water vapour and grease barrier properties of the self standing biohybrid films were determined in the various humidity conditions.

## 2. Experimental

### 2.1. Materials

*Pectin*. Sugar beet pectin (PE-2006-MB1) was obtained from Danisco Sugar A/S (Denmark). According to the manufacturer characteristics of the pectin were as follows: molecular weight 37 kDa, content of galacturonic acid 68%, degree of methylesterification 65% and degree of acetylation 25%.

*Nanoclay*. As an inorganic nanosized material in hybrid barrier films, a hydrophilic and unmodified aluminosilicate mineral from Aldrich was used. As reported by the manufacturer the purity of the montmorillonite was >98% with the aspect ratio of 150–200 and cation exchange capacity of 145 mequiv./100 g. Nanoclay was delivered as dry powder with the particle size of 5–25 μm.

### 2.2. Methods

#### 2.2.1. Dispergation of nanoclay and pectin/nanoclay fluids

*Nanoclay dispergation*. In order to ensure the sufficiently delaminated and nanosized structure of the nanoclay platelets, the nanoclay powder was dispersed in water in a concentration of 0.05% using either ultrasonic microtip (Branson Digital Sonifier) or high pressure fluidizer (Microfluidics M110Y). 10 min ultrasonic treatment with 25% power was used as a reference treatment for nanoclay homogenization studies conducted by fluidizer.

*Pectin solutions*. Aqueous solutions of sugar beet pectin were prepared into distilled water by mixing pectin and glycerol at final concentrations of 5 and 1.75 wt%, respectively. pH of the mixture was adjusted to pH 4.5 and the mixture was heated at 60 °C for 2 h to increase fluidity.

*Pectin/nanoclay dispersions*. 0.5, 1 or 2 wt% nanoclay was added to pectin solutions and immersed for two days under constant mixing. Fluidizer (Microfluidics M110Y) was used for homogenization of nanoclay/pectin dispersions. Feed solutions were pumped from inlet reservoir and pressurized by an intensifier pump to high pressure (900–1350 bars) and fed through fixed geometry chambers with inside microchannel diameter varying between 100 and 400 μm. Within the chambers high pressures forced pectin and nanoclays to form turbulent and opposing jets, which contributed to mixing in nanometer scale, minimizing diffusion limitation.

#### 2.2.2. Preparation of pectin/nanoclay films

*Model surfaces*. Nanoclay-pectin hybrid film formation and high shear induced orientation of nanoclay platelets were investigated by means of model surfaces which were prepared using high shear spincoating method with WS400BNPP Spincoater from Laurell Technologies Corporation. In spincoating technique the layer is deposited on the solid surface from the solvent by spinning the surface with high speed. The thin model layer enables the characterization of the fine structure of the materials by e.g. high resolution microscopic techniques. In addition, due to the high

shear spinning, the information on the orientation of the particles can be achieved. The both ultrasonic treated and fluidized aqueous dispersions of pure nanoclay as well as hybrid mixtures of pectin and nanoclay were spincoated on a polyvinyl amine premodified silica surface using fast spinning (2800 rpm for 1 min with the slow acceleration speed). The sufficient attachment of the nanoclay platelets on the silica surface was ensured with the heat treatment conducted at 80 °C for 1 h.

*Barrier films*. Pure pectin films and the films of fluidized hybrid films of pectin and nanoclay were prepared by casting 15 mL of each solution in polystyrene Petri dish (⌀ 8.5 cm) and dried for two days at room temperature. The obtained films were stored at room temperature and 50% relative humidity prior to further analyses. Final nanoclay concentrations in the solvent cast hybrid films were ~10, ~20 and ~30 wt%.

#### 2.2.3. Characterisation of dispersions and films

*Structural characterization with AFM and SEM*. A Nanoscope IIIa Multimode scanning probe microscopy, from Digital Instruments Inc., Santa Barbara, CA, USA, was used to determine the morphology and to estimate the height of the nanoclay platelets after ultrasonic or fluidizer treatments. Images were taken from the spincoated model surfaces in tapping mode in air using silicon cantilevers (Pointprobes, type = NCH) delivered by Nanosensors, Neuchald, Switzerland. No image processing except flattening was made.

Structures of the model surfaces and films were also analyzed using scanning electron microscopy (SEM, LEO DSM 982 Gemini FEG-SEM). The solvent cast barrier film samples (~10 mm × 10 mm) were attached on carbon adhesive discs (12 mm ⌀) pressed on 12.5 mm (⌀) aluminum stubs. Typically, no conductive coating was applied on the specimen prior to SEM imaging. However, in some cases a thin layer (~10 nm) of Platinum was sputter coated on the film surface to improve conductivity and stability of the specimen. The SEM analyses of the samples were conducted using electron energies of 1.0 keV and 2.0 keV. The reference pectin film was imaged at 0.5 keV electron energy using "TV-rate" scanning to avoid electron beam induced damage of the film.

*Optical profilometry*. Wyko NT9100 Optical Profiling System was used to visualize the three-dimensional topography and to determine the roughness average ($R_a$) of the solvent cast pectin films. Top side of the film surfaces, which had been exposed to air during drying, was measured.

*XRD* X-ray diffraction was used to determine the interlayer distance of layered nanoclays and pectin nanocomposites. Interlayer distances were calculated by the Bragg's Law: $2d \sin\theta = \lambda$, where $d$ is the interlayer distance, $\theta$ is the diffraction angle and $\lambda$ is the wavelength of the X-rays. X-ray powder diffraction patterns from the samples were run using Philips X'Pert MPD diffractometer using Cu X-ray tube ($\lambda$ = 1.542 Å).

#### 2.2.4. Barrier properties of the pectin/nanoclay films

*WVTR*. Water vapour transmission rates of the barrier films were determined gravimetrically using a modified ASTM E-96 procedure. Samples with a test area of 25 $cm^2$ were mounted on a circular aluminium dish (H.A. Büchel V/H, A.v.d. Korput, Baarn-Holland 45M-141), which contained water. Dishes were stored in test conditions of 23 °C and 50% relative humidity and weighed periodically until a constant rate of weight reduction was attained.

*OTR*. Oxygen transmission measurements were performed with Oxygen Permeation Analyser Model 8001 (Systech Instruments Ltd. UK). The tests were carried out at 23 °C and 0%, 50% and 80% relative humidity.

*Grease resistance*. Grease resistance was determined according to modified Tappi T 507 method. First, standard olive oil was colored with Sudan II dye and applied onto 5 cm × 5 cm sized blotting paper. Stain saturated piece of blotting paper was placed against the films and a piece of blank blotting paper (stain absorber) was placed against the other side. The whole stack was pressed between two plates and kept in oven at 60 °C for 4 h. At the end of the test period, the assembly was removed and the stain absorbers were examined. For each absorber the area and the number of stained spots, if any, were determined.

## 3. Results and discussion

### 3.1. Structural characteristics of the materials—model surface study

In order to investigate the structure of the individual nanoclay platelets, nanoclay powder, which consisted of agglomerated particles prior to delamination (Fig. 1a), was dispersed in water with the aid of ultrasonic microtip. Fine structure of the round particles, imaged using higher magnification, clearly reveals the laminar units on the particle surface. Fig. 1b shows how the aggregated structure is unraveled after ultrasonic dispersing. Individual nanoclay platelets spincoated on the silica surface are evenly distributed and the lateral dimensions of the platelets vary from tens of nanometers up to 500 nm.

Nanoclay delamination with the ultrasonic treatment was used for the reference purposes since this method is widely used for effective clay/water suspension preparation in a laboratory scale (Bae et al., 2009; Chen, Hao, Guo, Song, & Zhang, 2002; Shabeer, Chandrashekhara, & Schuman, 2007; Vaia, Jant, Kramer, & Giannelis, 1996). However, when considering larger scale preparation methods for hybrid materials and more even distribution of inorganic nanoparticles into a gel-like polymeric matrix, the sufficient homogeneity together with nanosized fine structure may not be achieved by ultrasonic treatment only. Therefore, the possibility of the high pressure fluidizer was investigated in order to delaminate the nanoclay and disperse it first into water and then into a continuous pectin matrix.

The thin spin coated model layers of nanoclay and hybrid materials of pectin and nanoclay enable the characterization of the fine structure of such materials by e.g. high resolution microscopic techniques. In addition, due to the high shear spinning, the information on the orientation of the individual particles and particles dispersed in a continuous polymer matrix can be achieved.

Fig. 1c shows the structure of nanoclay platelets which are spin coated on the silica surface from the aqueous dispersion after the high pressure fluidizer treatment. An even layer of laminar nanoclay particles with the similar size distribution as compared to the particles after ultrasonic treatment can be achieved. Thus, high pressure fluidizer treatment can be used as an efficient method to delaminate the nanoclay particles.

The thickness of the nanoclay platelets spin coated on the silica surface after ultrasonic or fluidizer treatment was estimated by AFM (Fig. 2a and b). From the AFM topography images, the height of the stacks formed by single nanoclay platelets can be determined. Z-range of the ultrasonic treated and fluidizer treated model surfaces is 16 nm and 20 nm, respectively. It seems that most of the nanoclay platelets are in the thickness range of 10 nm indicating stacks consisting of approximately 10 montmorillonite layers. Besides the information on the topography, the uniformity of the formed nanoclay model surface can be achieved from the AFM phase contrast images. Phase contrast images suggest that the surface is evenly covered by the nanoclay particles which are oriented laterally on the solid surface.

Three different loadings of nanoclay (0.5, 1 and 2 wt%) were dispersed into an aqueous solution of pectin at pH 4.5. The solutions were homogenized with the high pressure fluidizer in a similar

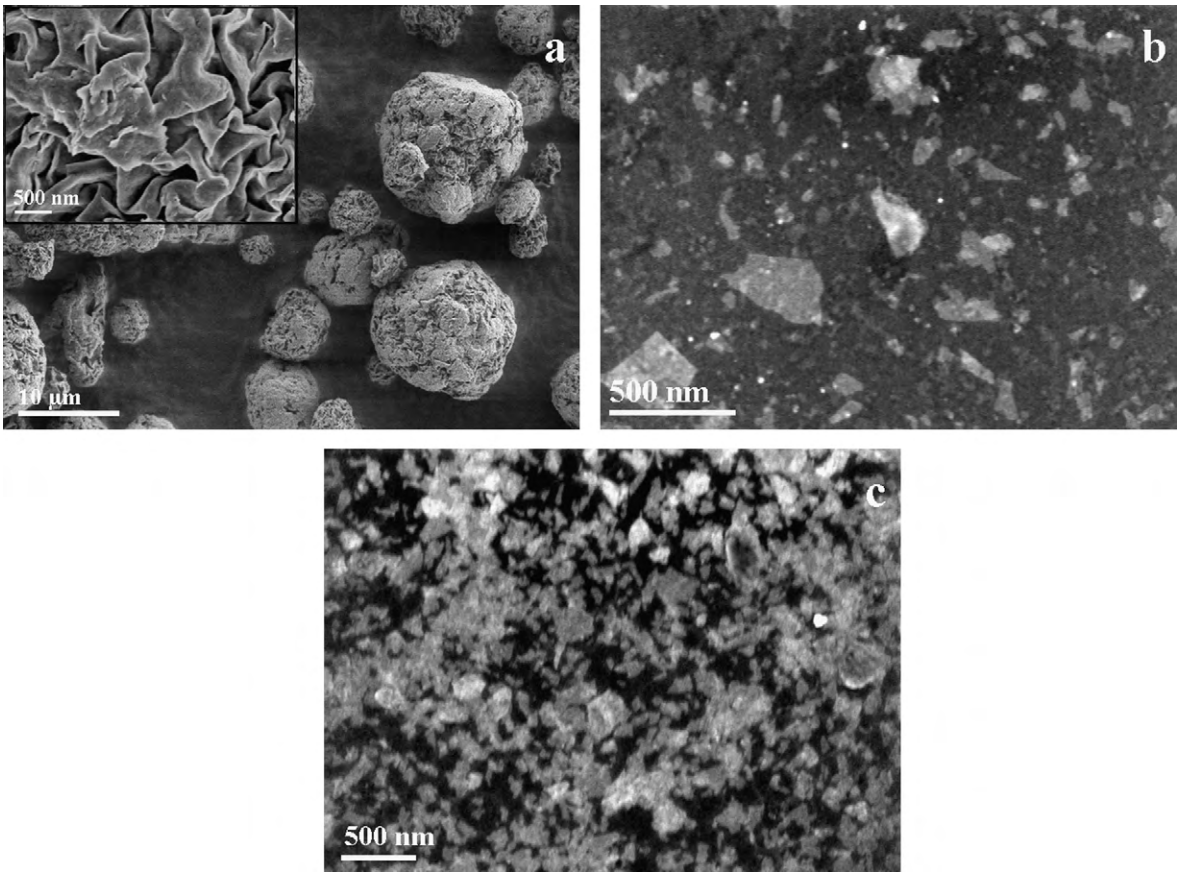


**Fig. 1.** SEM images of (a) large undispersed nanoclay aggregates. The excerpt shows the surface structural features: Laminar fine structure can been seen on the aggregate surfaces, (b) spincoated nanoclay platelets after dispersing with the ultrasonic microtip, and (c) spincoated nanoclay platelets after high pressure fluidizer treatment.

manner as the pure aqueous dispersions of nanoclay described above. Fluidized hybrid solutions were instantly spin coated on the silica surface in order to characterize the hybrid material fine structure.

Fig. 3 shows the structure of the spin coated hybrid layer of pectin and nanoclay in which the nanoclay content is at its highest (~30 wt%). Again, an even layer of laterally oriented nanoclay platelets can be seen with the 2D-dimensions of up to 500 nm. By the fluidizer treatment, the nanoclay platelets can be uniformly distributed into the pectin matrix.

The thickness determination by AFM was unsatisfactory due to the sticky nature of the pectin film (results not shown). While scanning the pectin containing layers, the pectin instantaneously contaminated the AFM tip which prevented the detailed structural characterisation. However, the comparison of the SEM images of the pure fluidized nanoclay platelets (Fig. 1c) and fluidized pectin-nanoclay hybrid material (Fig. 3) facilitates the assumption that the nanoclay is similarly delaminated, dispersed and oriented.

In an acidic medium an excess of protons creates positively charged clay edges (Tournassat et al., 2003a, 2003b) which leads to aggregation of the clay platelets due to the attractive interaction towards the negatively charged clay faces. These aggregates form so-called card-houses by edge(+)/face(−) contacts. At pH < 6 nanoclay dispersions coagulates easily already at low ionic strength since the electrostatic repulsive forces are weak and they are effectively screened by the presence of salt ions. However, although the studied system contained ions (none of the materials was purified) and the pH was low, it seems that nanoclay card-houses were effectively destructed due to the high shear fluidization. In addition, the negatively charged pectin polymers, when adsorbing on the positively charged nanoclay edges, may create a steric hindrance around the edges of the nanoclay stacks resulting in a stable and even hybrid structure.

### 3.2. Structural properties of the pectin/nanoclay solvent cast barrier films

In order to investigate the barrier properties of the hybrid materials, the films with the thickness of $100 \pm 10$ μm were prepared by solvent casting the fluidized dispersions. Sugar beet pectin without the nanoclay addition formed a slightly brownish and opaque film whereas the nanoclay containing films were brownish and transparent.

Fig. 4 shows the pure solvent cast pectin barrier film and barrier hybrid film of pectin with high loading (~30 wt%) of nanoclay. Pure pectin film is smooth and rather featureless (Fig. 4a) whereas the oriented nanoclay platelets dispersed into the pectin matrix can be clearly seen in Fig. 4b. The surface topography determination by optical profilometry reveals that the nanoclay addition does not roughen the film surface. On the contrary, the average roughness value, $R_a$, is higher for pure pectin film compared to the hybrid film with the high loading of nanoclay. The average roughness values for pure pectin film and hybrid film of pectin with ~30 wt% of nanoclay were 380 nm and 160 nm, respectively. High surface roughness value for pure pectin film is due to the humidity conditions in which the topography determinations were conducted (50% RH). The film surface roughening by the humid conditions seems to be prevented by the nanoclay addition.

Intercalated structures are formed when polymeric chains are intercalated between the silicate layers (Pavlidou & Papaspyrides, 2008) The result is a well ordered multilayer structure of alternating polymeric and inorganic layers, with a repeat interlayer distance

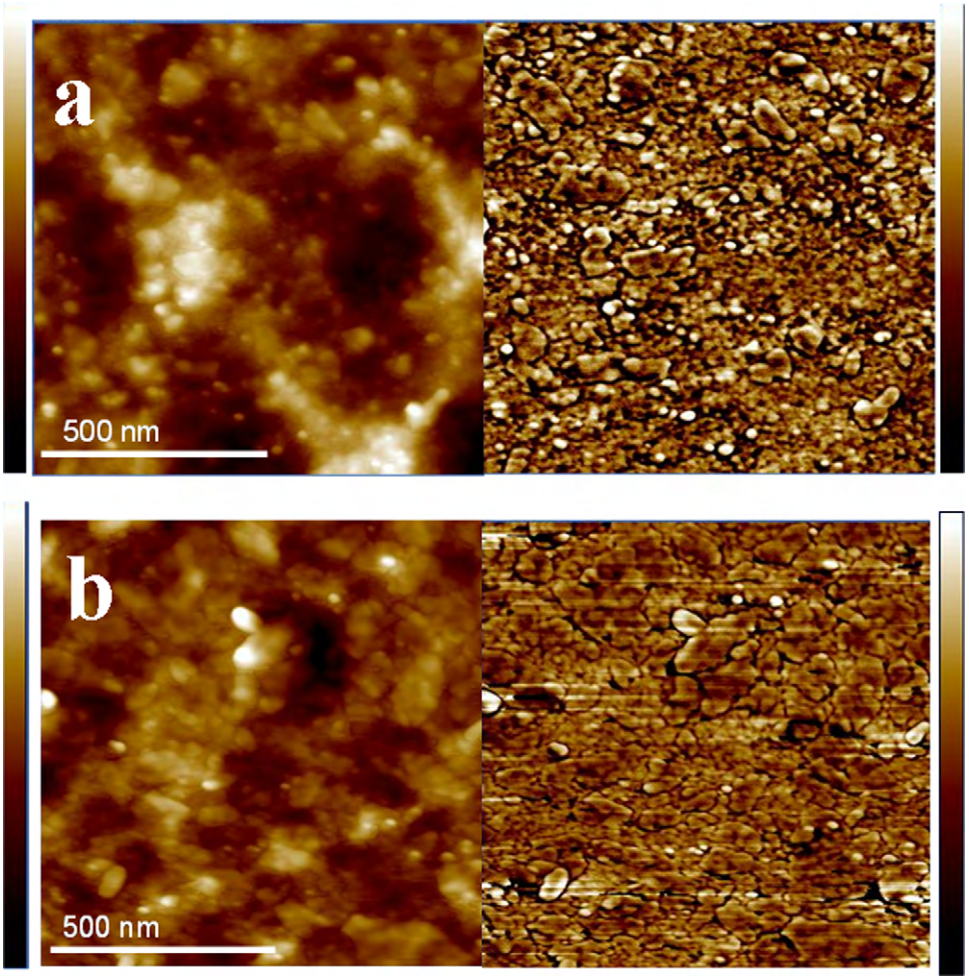


**Fig. 2.** (a) AFM topography image (left) and phase contrast image (right) of spincoated nanoclay platelets after dispersing with the ultrasonic microtip. The sample is the same model surface as imaged with SEM in Fig. 1b. Z-range scale bars are 16 nm and 40°, respectively. (b) AFM topography image (left) and phase contrast image (right) of spincoated nanoclay platelets after high pressure fluidizer treatment. The sample is the same model surface as imaged with SEM in Fig. 1c. Z-range scale bars are 20 nm and 45°, respectively.

(*d*-value) between them. The interlayer distance (*d*-value) of the stacked nanoclays was measured by XRD using the Braggs's law.

Fig. 5 shows the recorded X-ray diffractograms of the produced nanocomposite films as well as of the used montmorillonate nanoclay powder. The diffractogram measured from the pure pectin film is also reproduced in the image. The silicon curve is from the amorphous silicon that was used as supporting substrate for the composite films.

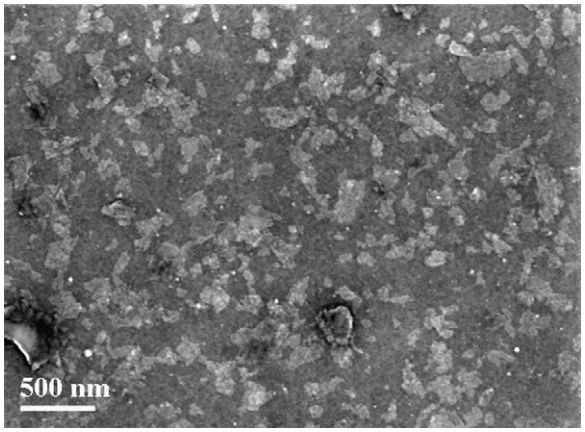


**Fig. 3.** SEM image of a spincoated hybrid material of nanoclay and pectin after the high pressure fluidizer treatment. Spincoating is conducted from the hybrid solution containing high load (~30 wt%) of nanoclay.

The pristine powdery nanoclay had an interlayer distance of 1.23 nm ($2\theta = 7.19$). By fluidization the *d*-values of ~10, ~20 and ~30 wt% nanoclay containing films were increased to about 2.01 nm ($2\theta = 4.41$), 1.96 nm ($2\theta = 4.51$) and 1.82 nm ($2\theta = 4.86$), respectively. The increase in *d*-values is attributed to the water intake of the montmorillonate clay platelets. Thus, the observed slightly increased interlayer distance is due to the swelling of the nanoclay platelets rather than the formation of intercalated film structure. The increase in *d*-value is indeed insufficient for pectin molecules to intercalate within the nanoclay interlayers. In addition, the repulsive forces between anionic nanoclay faces and anionic pectin molecules further hinder the migration of pectin within the layers. Furthermore, as silanol edges have positive charges in acidic conditions, they may positively interact with pectin chains and form branchy structures around the nanoclay stacks (Perez, Flores, Marangoni, Gerschenson, & Rojas, 2009; Wang, Shen, Zhang, & Tong, 2005).

### 3.3. Barrier properties of the pectin/nanoclay films

Water vapour transmission results indicate that nanoclay addition improves the barrier properties of the pectin film (Fig. 6). The

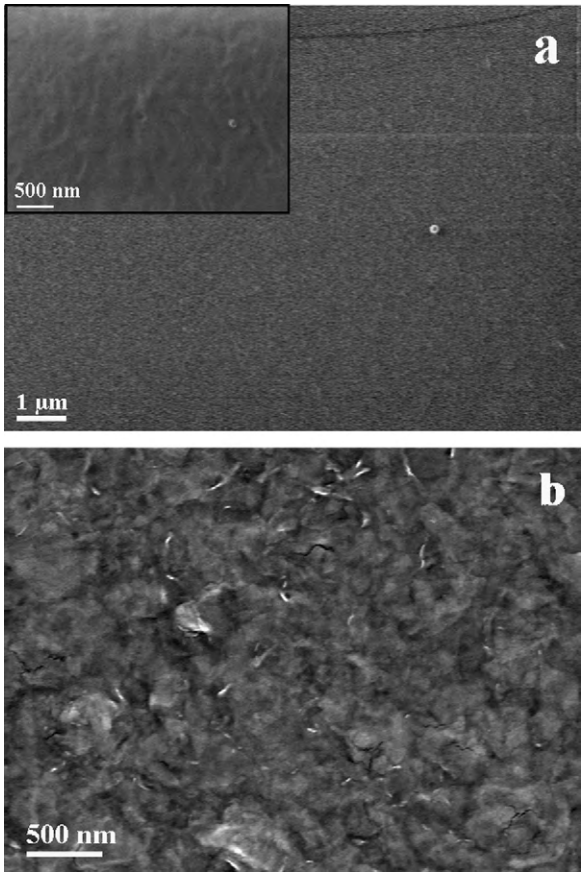


**Fig. 4.** SEM images of (a) pure solvent cast pectin barrier film (magnification 10,000×). The excerpt shows the rather featureless film surface in higher magnification (30,000×), (b) solvent cast hybrid film of pectin and nanoclay. The dry film contains ~30 wt% of nanoclay.

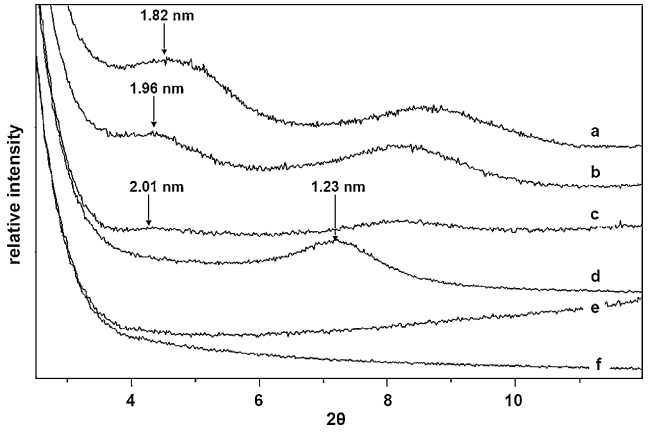


**Fig. 5.** XRD-patterns of solvent cast barrier films of pectin containing (a) ~30 wt%, (b) ~20 wt%, (c) ~10 wt% of nanoclay. As a reference materials curve (d) corresponds to nanoclay powder, (e) pure pectin film without nanoclay addition, and (f) silicon baseline.

similar kind of behaviour was found with starch/clay nanocomposites where the increasing clay content also led to an improvement in water vapour barrier properties (Park, Lee, Park, Cho, & Ha, 2003). In high humidity conditions nanoclay plates absorb water and swell, but they still form single individual barrier layers against vapour transmission. At the same time the penetrating water molecules effectively plasticize and swell the matrix polymer. However, the water soluble pectin is lacking the capability to fully prevent the water vapour transmission, and thus, total barrier effect of films

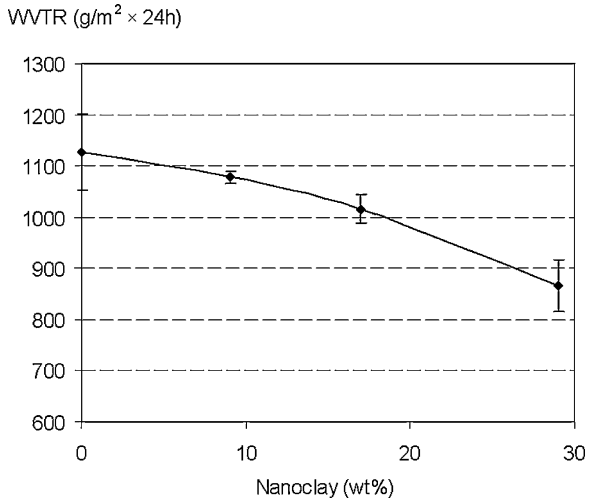


**Fig. 6.** Water vapour transmission rates of solvent cast hybrid films of pectin films with different amounts of nanoclay.

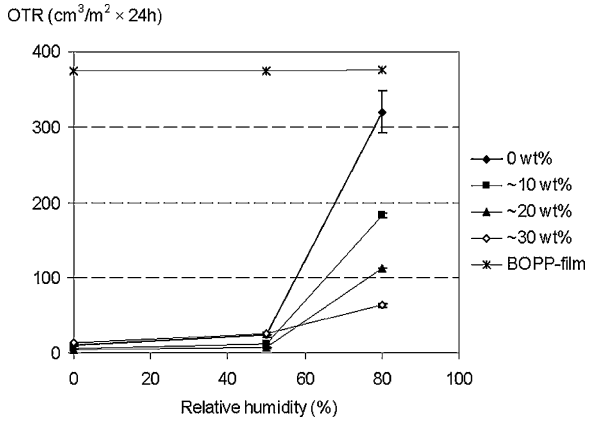


**Fig. 7.** Oxygen transmission rates of solvent cast hybrid films of pectin films with different amounts of nanoclay. BOPP is commercial biaxially oriented polypropylene film of which oxygen transmission is normalized to film with 100 μm thickness (Vartiainen et al., 2008).

with ~30 wt% nanoclay is not more than 23%. According to the literature, in the case of more hydrophobic PLA nanocomposites, the clay incorporation decreased the water vapour transmission of the films by 40–50% (Thellen et al., 2005).

Nanoclay addition clearly improved the oxygen barrier properties of the pectin film also in high humidity conditions (Fig. 7). Oxygen transmission rate was reduced over 80% with pectin films containing ~30 wt% of nanoclay when compared to the film of pure pectin. These results are consistent with other studies (Chang, Uk-An, & Sur, 2003; Ke & Yongping, 2005; Ray, Yamada, Okamoto, & Ueda, 2003) where 15–88% reduction in oxygen transmission rates has been attained with PET and PLA-based layered silicate nanocomposites. The oxygen and water vapour transmission rates were also comparable with the results of films produced by ball milling of pectin and natural montmorillonite clay (Mangiacapra et al., 2006). Achieved oxygen barrier properties of nanoclay containing pectin films are significantly better in high humidity conditions as compared with the commercial polyolefin films of the same thickness (Vartiainen, Rättö, Lantto, Nättinen, & Hurme, 2008).

Bentonite clays have a capability to absorb oils and greases (Lagaly, 1995). However, pectin itself formed an excellent barrier against grease and the nanoclay addition did not change this feature anyhow (results not shown). As a result of the grease resistance determinations, all of the films were totally impermeable to grease

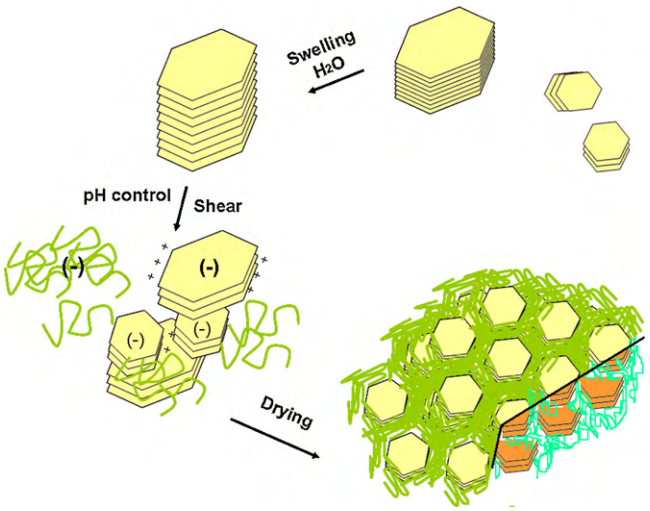


**Fig. 8.** Schematic illustration of the structural features of the sufficiently delaminated nanoclay platelets dispersed in a continuous pectin matrix. Due to the high shear, the nanoclay platelets disintegrates into a stacks consisting of approximately 10–15 individual nanoclay platelets. Pectin matrix glues stacks into a laterally organized films and in addition it prevents the stacks to agglomerate in acidic pH.

under the conditions tested. Hydrogen bonds in pectin evoke excellent barrier against grease and when forming a continuous matrix it totally prevented the grease penetration.

Barrier improvements are explained using tortuous path theory which relates to the alignment of the nanoclay platelets. As a result of the sufficient delamination, the effective path length for molecular diffusion increases and the path becomes highly tortuous to reduce the effect of gas transmission through the film (Christopher & Lerner, 2001). In high humidity conditions water molecules penetrate into pectin films and destroy the hydrogen bonded structure and weaken the barrier properties.

## 4. Conclusions

Nanoclay was successfully dispersed in an aqueous pectin solution using high pressure fluidizer in acidic conditions. The structural characterization of the hybrid layers via model surfaces facilitates the reasoning the mechanisms behind the material properties to act as a barrier. Fig. 8 proposes the formation and the final structure of the hybrid material of sugar beet pectin and montmorillonite. Instead of the full exfoliation, the stacks of 10–15 nm thick swelled nanoclay layers are formed during the high shear fluidization. Anionic pectin interacts with the cationic edges of the nanoclay stacks; it bonds the stacks into a laterally oriented film and prevents the nanoclay agglomeration. These hybrid films showed significantly improved barrier properties against oxygen. In addition, the ability to prevent the water vapour transmission was slightly increased and, furthermore, the films were totally impermeable to grease. The developed biohybrid material can be potentially exploited as a safe and environmentally sound alternative for synthetic barrier packaging materials. Due to the exploited pH conditions, the further film modifications by enzymatic cross-linking allow the introduction of supplementary material properties.

## References


Arora, A., & Padua, G. W. (2010). Review: Nanocomposites in food packaging. *Journal of Food Science*, *75*, 43–48.

Bae, H. J., Park, H. J., Darby, D. O., Kimmel, R. M., & Whiteside, W. S. (2009). Development and characterization of PET/fish gelatin-nanoclay composite/LDPE laminate. *Packaging Technology and Science*, *22*, 371–383.

Blumstein, A. (1965). Polymerization of adsorbed monolayers. 1. Preparation of the clay-polymer complex. *Journal of Polymer Science Part A: Polymer Chemistry*, *3*, 2653–2664.

Chang, J.-H., Uk-An, Y., & Sur, G. S. (2003). Poly(lactic acid) nanocomposites with various organoclays. I. Thermomechanical properties, morphology, and gas permeability. *Journal of Polymer Science, Part B: Polymer Physics*, *41*, 94–103.

Chen, G. X., Hao, G. J., Guo, T. Y., Song, M. D., & Zhang, B. H. (2002). Structure and mechanical properties of poly(3-hydroxybutyrate-co-3-hydroxyvalerate) (PHBV)/clay nanocomposites. *Journal of Material Science Letters*, *21*, 1587–1589.

Christopher, O. O., & Lerner, M. (2001). *Nanocomposites and intercalation compound* (3rd ed.). *Encyclopedia of Physical Science and Technology*. Reproduced in part with permission from Elsevier 2006.

Hansen, N., & Plackett, D. (2008). Sustainable films and coatings from hemicelluloses: A review. *Biomacromolecules*, *9*, 1493–1505.

Harrington, R. http://www.foodproductiondaily.com/Packaging/Strong-growth-in-nano-packing-forecast-but-Europe-still-cautious, 2009

Ke, Z., & Yongping, B. (2005). Improve gas barrier property of PET film with montmorillonite by in situ interlayer polymerization. *Materials Letters*, *59*, 3348–3351.

Kirby, A., MacDougall, A., & Morris, V. (2008). Atomic force microscopy of tomato and sugar beet pectin molecules. *Carbohydrate Polymers*, *71*, 640–647.

Lagaly, G. (1995). Surface and interlayer reactions: Bentonites as adsorbents. In G. J. Churchmann, R. W. Fitzpatrick, & R. A. Eggleton (Eds.), *Proceedings of 10th International Clay Conference, Adelaide, 1993* (pp. 137–144). Melbourne, Australia: CSIRO Publ.

Lagarón, J. M., & Fendler, A. (2009). High water barrier nanobiocomposites of methyl cellulose and chitosan for film and coating applications. *Journal of Plastic Film and Sheeting*, *25*, 47–59.

Lan, T., Kaviratna, P. D., & Pinnavaia, T. J. (1994). On the nature of polyimide-clay hybrid composites. *Chemistry of Materials*, *6*, 573–575.

Maksimov, R., Lagzdins, A., Lilichenko, N., & Plume, E. (2009). Mechanical properties and water vapour permeability of starch/montmorillonite nanocomposites. *Polymer Engineering and Science*, *49*, 2421–2429.

Mangiacapra, P., Gorrasi, G., Sorrentino, A., & Vittoria, V. (2006). Biodegradable nanocomposites obtained by ball milling of pectin and montmorillonites. *Carbohydrate Polymers*, *64*, 516–523.

Messersmith, P. B., & Giannelis, E. P. (1995). Synthesis and barrier properties of poly(ε-caprolactone)-layered silicate nanocomposites. *Journal of Polymer Science Part A: Polymer Chemistry*, *33*, 1047–1057.

Napierała, D., & Nowotarska, A. (2006). Water vapour transmission properties of wheat starch-sorbitol film. *Acta Agrophysica*, *7*, 151–159.

Pavlidou, S., & Papaspyrides, C. (2008). A review on polymer-layered silicate nanocomposites. *Progress in Polymer Science*, *33*, 1119–1198.

Park, H. M., Lee, W. K., Park, C. Y., Cho, W. J., & Ha, C. S. (2003). Environmentally friendly polymer hybrids: Part I-mechanical, thermal, and barrier properties of thermoplastic starch/clay nanocomposites. *Journal of Materials Science*, *38*, 909–915.

Perez, C. D, Flores, S. K., Marangoni, A. G., Gerschenson, L. N., & Rojas, A. M. (2009). Development of a high methoxyl pectin edible film for retention of L-(+)-ascorbic acid. *Journal of Agricultural and Food Chemistry*, *57*, 6844–6855.

Plackett, D., Holm, V., Johansen, P., Ndoni, S., Nielsen, P., Sipilainen-Malm, T., et al. (2006). Characterization of L-polylactide and L-polylactide–polycaprolactone co-polymer films for use in cheese-packaging applications. *Packaging Technology and Science*, *19*, 1–24.

Ray, S. S., Yamada, K., Okamoto, M., & Ueda, K. (2003). New polylactide/layered silicate nanocomposites 2. Concurrent improvements of material properties, biodegradability and melt rheology. *Polymer*, *44*, 857–866.

Shabeer, A., Chandrashekhara, K., & Schuman, T. (2007). Synthesis and characterization of soy-based nanocomposites. *Journal of Composite Materials*, *41*, 1825–1849.

Siew, C. K., & Williams, P. A. (2008). Role of protein and ferulic acid in the emulsification properties of sugar beet pectin. *Journal of Agricultural and Food Chemistry*, *56*, 4164–4171.

Thellen, C., Orroth, C., Froio, D., Ziegler, D., Lucciarini, J., Farrell, R., et al. (2005). Influence of montmorillonite layered silicate on plasticized poly(L-lactide) blown films. *Polymer*, *46*, 11716–11727.

Tournassat, C., Greneche, J.-M., Tisserant, D., & Charlet, L. (2003). The titration of clay minerals. I. Discontinuous backtitration technique combinedwith CEC measurements. *Journal of Colloid and Interface Science*, *273*, 224–233.

Tournassat, C., Ferrage, E., Poinsignon, C., & Charlet, L. (2003). The titration of clay minerals. II. Structure-based model and implications for clay reactivity. *Journal of Colloid and Interface Science*, *273*, 234–246.

Vaia, R. A., Jant, K. D., Kramer, E. J., & Giannelis, E. P. (1996). Microstructural evaluation of melt-intercalated polymer-organically modified layered silicate nanocomposites. *Chemistry of Materials*, *8*, 2628–2635.

Vartiainen, J., Rättö, M., Lantto, R., Nättinen, K., & Hurme, E. (2008). Tyrosinase-catalysed grafting of food-grade gallates to chitosan: Surface properties of novel functional coatings. *Packaging Technology and Science*, *21*, 317–328.

Vartiainen, J., Tuominen, M., & Nättinen, K. (2010). Biohybrid nanocomposite from sonicated chitosan and nanoclay. *Journal of Applied Polymer Science*, *116*, 3638–3647.

Vincken, J.-P., Schols, H., Oomen, R., McCann, M., Ulvskov, P., Voragen, A., et al. (2003). If homogalacturonan were a side chain of rhamnogalacturonan I. Implications for cell wall architecture. *Plant Physiology*, *132*, 1781–1789.

Wang, S. F., Shen, L., Zhang, W. D., & Tong, Y. J. (2005). Preparation and mechanical properties of chitosan/carbon nanotubes composites. *Biomacromolecules*, *6*, 3067–3072.

Yano, K., Usuki, A., & Okada, A. (1997). Synthesis and properties of polyimide-clay hybrid films. *Journal of Polymer Science Part A: Polymer Chemistry*, *35*, 2289–2294.

Zsivánovits, G., Marudova, M., & Ring, S. (2005). Influence of mechanical properties of pectin films on charge density and charge density distribution in pectin macromolecule. *Colloid & Polymer Science*, *284*, 301–308.